

Finite State Predictive Current and Common Mode Voltage Control of a Seven-phase Voltage Source Inverter

Atif Iqbal, Shaikh Moinoddin*, Khaliqur Rahman

Department of Electrical Engineering, Qatar University, Doha, Qatar

*Electrical Engineering Section, University Polytechnic, Aligarh Muslim University, Aligarh, India

Article Info

Article history:

Received May 16, 2015

Revised Aug 5, 2015

Accepted Aug 20, 2015

Keyword:

Common mode voltage

Current control

Model predictive control

Multi-phase

Seven-phase

ABSTRACT

The paper illustrates finite set predictive current control (FSPC) along with common mode voltage control of a seven-phase voltage source inverter (VSI). The current and common mode voltage (CMV) controls are done considering a finite set of control actions. The space vector model of a seven-phase voltage source inverter produces $2^7 = 128$ space voltage vectors, with 126 active and two zero vectors. Out of 126 space vectors 112 are distinct and 14 are redundant vectors. To control the current and the common mode voltage, specific set of space vectors are chosen that minimizes the magnitude of the CMV and makes it a dc signal and simultaneously track the reference current. Hence no common mode current can flow. Three sets of space vectors are used for switching actuation, in one case only 15 vectors are used (14 active and one zero), in second case 14 vectors are used, followed by use of 8 space vectors (7 large and one zero) and finally 7 large vectors are employed. Optimal algorithm is employed to find the vector which minimizes the chosen cost function. The effect of selecting the cost function, the number of space vectors on current tracking and common mode voltage is investigated and reported. The developed technique is tested for RL load using simulation and experimental approaches.

Copyright © 2015 Institute of Advanced Engineering and Science.
All rights reserved.

Corresponding Author:

Atif Iqbal

Departement of Electrical Engineering,

Qatar University,

PO Box 2713, Doha, Qatar

Email: atif.iqbal@qu.edu.qa

1. INTRODUCTION

In power electronic converter, the current control is considered as one of the important and crucial issue. Many literatures reported current control issues and several techniques are proposed over the years [1]. Traditional methods of current control are Hysteresis based control also called bang-bang control, carrier-based sinusoidal current control and current control based on space vectors approach [2]. Hysteresis current control is most simple method but it gives variable switching frequency and is difficult for digital realization. Ramp comparison PWM technique and space vector PWM approaches yield constant switching frequency operation. Hysteresis control offer variable switching frequency, however, it can be modified to generate constant switching frequency of the inverter legs [3]. Another approach of current control called 'model predictive current control' (MPC) is becoming more popular for applications in power electronics and electric drives. Since power converter generates many switching states and some of them are redundant and may not be useful in obtaining high performance dynamics. Hence, some of the switching states can be rejected and may not be employed for controls such control are called 'finite set model predictive control'. This technique has been employed in controlling three-phase power electronics converters and drives [4-9]. Inherently, MPC is computational intensive approach, however, due to the advent of fast digital signal processors, Field programmable gate arrays and microcontrollers it is now practically realizable approach for

complex systems such as power electronic converters and drives. The method of control is also attractive for multiphase motor drives and literature is available on utilizing MPC for five-phase two-level inverter [10-11], six-phase inverter [12-15], five-phase three-level NPC inverter [16] and seven-phase inverter [17].

Owing to inherent advantages of multi-phase machine, they are considered mainly in high power drive applications such as ship propulsion, electric and hybrid vehicles, 'more electric aircraft' etc [18]. Proper Pulse Width Modulation control techniques are needed to control the drive systems that are supplied by multi-phase inverters. Several PWM techniques are proposed and presented in the literature for multi-phase voltage source inverters [18-19].

The current control in multi-phase drive system is an extension of three-phase drive such as hysteresis control, carrier-based control, space vector based control and other non-linear controls [18], [20].

This paper proposes finite set model predictive current control of a seven-phase VSI feeding a RL load. The aim of the work is to develop current control approach along with common mode voltage control. The common mode voltage can be controlled by pre-selection of a set of space vector. The similar approach is employed for a five-phase VSI in [21]. The proposed approach is extension of method adopted for a five-phase VSI [10-11]. A seven-phase inverter generates $2^7 = 128$ space vectors and thus there is greater degree of freedom in choosing proper space vector combination for implementing the control algorithm [22]. This paper proposes an algorithm based on a choice of 14 active and one zero, 14 active, 7 active and one zero and 7 active while the total set of vectors are 128. Reduced number of space vectors are used since it is easier for the real time implementation and control of common mode voltage.

2. FINITE STATE PREDICTIVE CURRENT CONTROL

2.1. The Control Strategy

The current control suggested in this paper is based on the finite set model predictive approach. The power converter yield $2^7 = 128$ switching states, however, for the current control, reduced switching states are utilized and hence called 'finite set' MPC. A block diagram to show the principle of the proposed strategy is depicted in Figure 1. The discrete load model called 'Predictive Model' is used to pre-calculate the trajectory of the load current in the next sampling interval assuming the known current in the present sample. The pre-calculated current sample is then fed to the optimizer along with the commanded current (obtained from the external user controlled loop). The optimizer calculates the cost function for all the possible switching combinations of the inverter (note that smaller set of vectors are chosen). Thus, it generates the optimal switching state corresponding to the global minimum cost function in each sampling interval and passes it on to the gate drive of the inverter. This is how the optimal current control solution is obtained. The technique of model predictive control concept is different from the traditional pulse width modulation method. In traditional PWM the symmetrical switching patterns are generated and it is ensured that each leg changes the state at-least twice in the same switching interval. This ensure constant switching frequency spectrum of the load current. Contrary to this, in the model predictive control approach there is no fixed switching pattern and hence the spectrum shows variable switching frequency. However, MPC approach is very powerful being simple and intuitive. The controller can incorporate many desired control features and can met several control objectives by simple modification of the cost function. The cost function can incorporate other control features such as reduced switching losses, lower switch stress, number of switch commutation etc.

A seven-phase voltage source inverter yield large number of space vectors (126 active and 2 zero), several possible solutions could exist to implement model predictive control. Many control objectives can be met with flexible control. Nevertheless, in this paper three different solutions are investigated and reported. However, there still remain many more to explore.

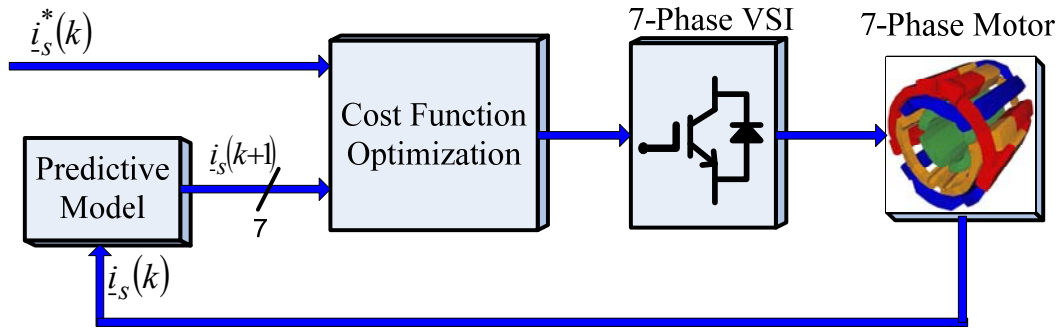


Figure 1. Model predictive control blocks schematic

2.2. The Cost Function

The choice of the cost function is the most important and crucial step of the model predictive control. An intelligent choice leads to the optimal solution of the control objectives. Thus, the cost function should include all the parameters to be optimized within the imposed constraints. In the current control the most important variable is the current tracking error. Thus the most simple and straight forward choice is the absolute value of the current error. The other choices could be square of the current error, integral of the current error, the rate of change of error etc. In this paper, square of the absolute error is chosen. Specifically in a seven-phase drive system there exist three orthogonal subspaces namely α - β and x_1 - y_1 and x_2 - y_2 . Thus in case of a seven-phase drive system the current errors in all the three planes have to be considered for devising a cost function. In general, for current error, the cost function is given as;

$$\begin{aligned} \hat{g}_{\alpha\beta} &= |i_{\alpha}^*(k) - \hat{i}_{\alpha}(k+1)| + |i_{\beta}^*(k) - \hat{i}_{\beta}(k+1)| \\ \hat{g}_{x_1y_1} &= |i_{x_1}^*(k) - \hat{i}_{x_1}(k+1)| + |i_{y_1}^*(k) - \hat{i}_{y_1}(k+1)| \\ \hat{g}_{x_2y_2} &= |i_{x_2}^*(k) - \hat{i}_{x_2}(k+1)| + |i_{y_2}^*(k) - \hat{i}_{y_2}(k+1)| \end{aligned} \quad (1)$$

The final cost function can be expressed as;

$$J_{\alpha\beta x_1y_1x_2y_2} = \mu \|\hat{g}_{\alpha\beta}\|^2 + \gamma \|\hat{g}_{x_1y_1}\|^2 + \delta \|\hat{g}_{x_2y_2}\|^2 \quad (2)$$

Where $\|\cdot\|$ denote modulus and μ , γ & δ are tuning parameters that offers degree of freedom to put emphasis on $\alpha - \beta$ or $x_1 - y_1$, or $x_2 - y_2$ subspaces. Comparative studies are made to emphasize the effect of choice of the tuning parameter on the performance of the controller.

2.3. Seven-phase Voltage Source Inverter Model

Power circuit topology of a seven-phase VSI feeding a RLE load is shown in Figure 2. The inverter input DC voltage is regarded further on as being constant. The inverter output phase voltages are denoted in Figure 2 with lower case symbol (a, b, \dots, g), while the leg voltages have symbols in capital letters (A, B, \dots, G). The model of seven-phase VSI is developed in space vector form in [23], assuming an ideal commutation and zero forward voltage drop. A brief review is presented here.

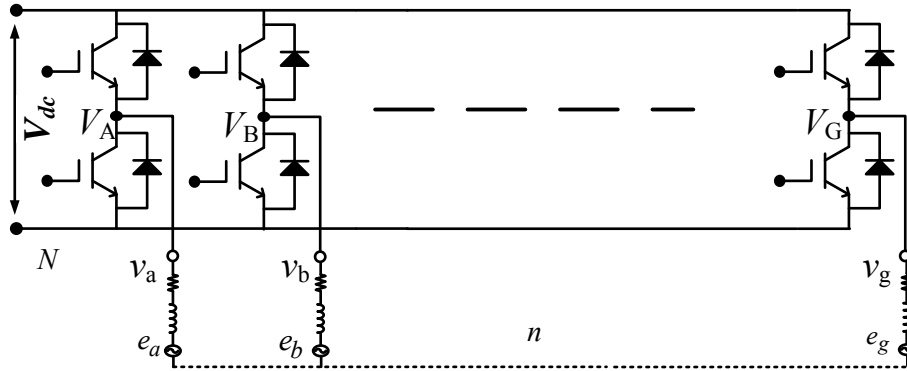


Figure 2. Power circuit of a seven-phase VSI

The relationship between the inverter phase-to-neutral voltages and inverter pole voltages is obtained as;

$$\begin{aligned}
 v_a &= (6/7)v_A - (1/7)(v_B + v_C + v_D + v_E + v_F + v_G) \\
 v_b &= (6/7)v_B - (1/7)(v_A + v_C + v_D + v_E + v_F + v_G) \\
 v_c &= (6/7)v_C - (1/7)(v_A + v_B + v_D + v_E + v_F + v_G) \\
 v_d &= (6/7)v_D - (1/7)(v_A + v_B + v_C + v_E + v_F + v_G) \\
 v_e &= (6/7)v_E - (1/7)(v_A + v_B + v_C + v_D + v_F + v_G) \\
 v_f &= (6/7)v_F - (1/7)(v_A + v_B + v_C + v_D + v_E + v_G) \\
 v_g &= (6/7)v_G - (1/7)(v_A + v_B + v_C + v_D + v_E + v_F)
 \end{aligned} \tag{3a}$$

where the inverter pole voltages take the values of $\pm 0.5V_{dc}$. The common mode voltage is defined as:

$$V_{nN} = -\frac{v_A + v_B + v_C + v_D + v_E + v_F + v_G}{7} \tag{3b}$$

And common mode current is defined as the current flowing through the stray capacitance:

$$i_{nN} = C_{stray} \frac{dV_{nN}}{dt} \tag{3c}$$

Hence the common mode current can be reduced by reducing the rate of change of the common mode voltage. The common mode voltage can be eliminated completely if the rate of change of common mode voltage is made zero or in other words if the common mode voltage is made dc. In this paper, the common mode voltage is made dc by choosing a specific set of the space vectors as discussed in the next section.

In general, an n phase two level VSI yield a total of 2^n number of switching states. Therefore, for a seven-phase VSI, total number of switching states are 128, in which two are zero vectors and the remaining 126 are active vectors. By using decoupling transformation matrix given in equation (4b) each voltage vector can be decomposed into three orthogonal two dimensional subspaces $d-q, x_1-y_1$ and x_2-y_2 (assuming isolated neutral and hence no zero sequence component).

In case of a seven-phase VSI, total switching combination of 128 numbers yield same number of switching space voltage vectors. Out of these 128 space voltage vectors, 126 are active and two are zero space vectors and they form nine concentric polygons of fourteen sides in $d-q$ plane with zero space vectors at the origin as shown in Figure 3.

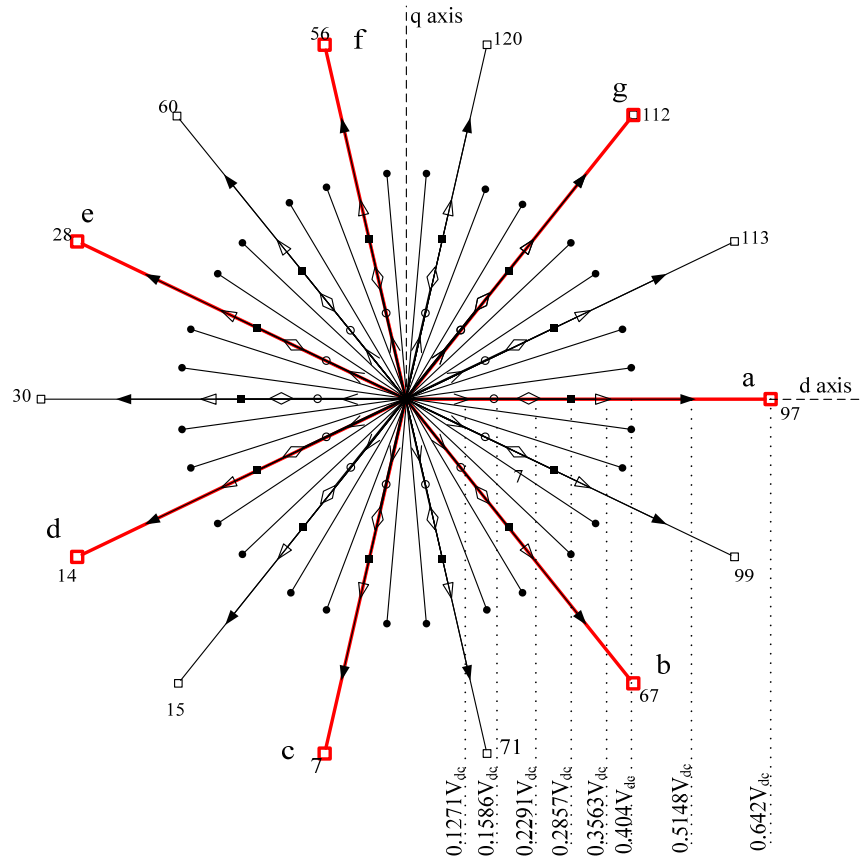


Figure 3. Phase-to-neutral voltage space voltage vectors (states 0 and 128 are at origin) in d - q plane

However, since a seven-phase system is under consideration, one has to represent the inverter space vectors in a seven-dimensional space. Such a space can be decomposed into three two-dimensional sub-spaces (d - q , x_1 - y_1 and x_2 - y_2) and one single-dimensional sub-space (zero-sequence). Since the load is assumed to be star-connected with isolated neutral point, zero-sequence cannot be excited and it is therefore sufficient to consider only three two-dimensional sub-spaces, d - q , x_1 - y_1 and x_2 - y_2 . Inverter voltage space vector in d - q sub-space is given with [20],

$$\underline{v}_{dq} = (2/7) \left(v_a + a v_b + a^2 v_c + a^3 v_d + a^4 v_e + a^5 v_f + a^6 v_g \right) \quad (4a)$$

where $a = e^{j2\pi/7}$, $a^2 = e^{j4\pi/7}$, $a^3 = e^{j6\pi/7}$, $a^4 = e^{j8\pi/7}$, $a^5 = e^{j10\pi/7}$, $a^6 = e^{j12\pi/7}$

Inverter voltage space vectors in the second two-dimensional sub-space (x_1 - y_1) and the third two-dimensional sub-space (x_2 - y_2) are determined with,

$$\begin{aligned} \underline{v}_{x_1 y_1} &= (2/7) \left(v_a + a^2 v_b + a^4 v_c + a^6 v_d + a v_e + a^3 v_f + a^5 v_g \right) \\ \underline{v}_{x_2 y_2} &= (2/7) \left(v_a + a^3 v_b + a^6 v_c + a^2 v_d + a^5 v_e + a v_f + a^4 v_g \right) \end{aligned} \quad (4b)$$

The phase voltage space vectors in three orthogonal planes, obtained using (1), are shown in Figures 3-5. It can be seen from Figures 3-5 that the outer most i.e. first, second, third, fourth, fifth, sixth, seventh, and eighth tetra-decagons space vectors of the d - q plane map into the sixth, eighth, third, second, fifth, seventh, first and fourth of the tetra-decagon of the x_1 - y_1 plane respectively; and seventh, fourth, third, eighth, fifth, first, sixth and second of the tetra-Decagon of the x_2 - y_2 plane respectively. To show this mapping same symbolic representation are used for the same group of space vectors. Further, it is observed from the above mapping that the phase sequence a, b, c, d, e, f & g of d - q plane corresponds to a, c, e, g, b, d, f of x_1 - y_1 plane (third harmonic) and a, d, g, c, f, b, e of x_2 - y_2 plane (fifth harmonic), respectively.

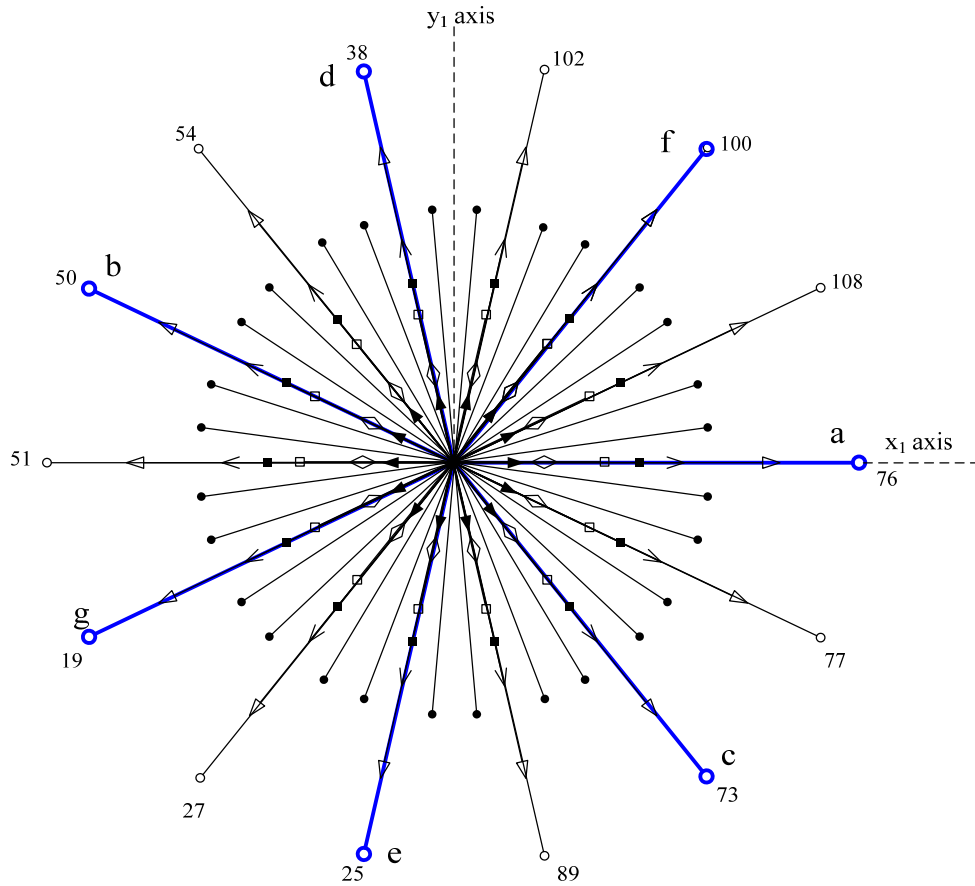


Figure 4. Phase-to-neutral voltage space vectors for states 1-128.(states0-128 are at origin) in x_1 - y_1 plane

2.4. Discrete Load Model

The load is assumed as a seven-phase RL (Resistance and, inductance). The discrete time model of the load suitable for current prediction is obtained from [67];

$$\hat{\underline{i}}(k+1) = \frac{T_s}{L} (\underline{v}(k)) + \underline{i}(k) \left(1 - \frac{RT_s}{L} \right) \tag{5}$$

Where R and L are the resistance and inductance of the load, T_s is the sampling interval, \underline{i} is the load current space vector, \underline{v} is the inverter voltage space vector used as a decision variable.

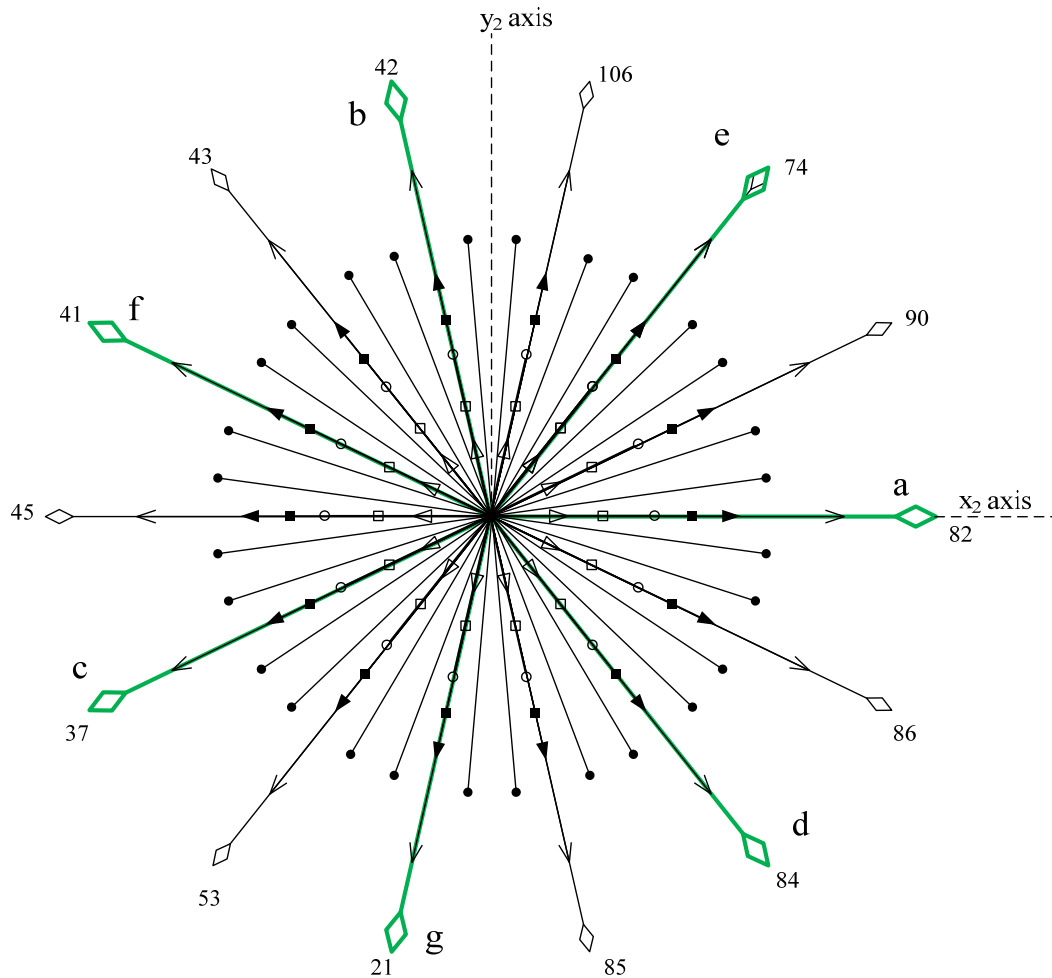


Figure 5. Phase-to-neutral voltage space vectors for states 1-128 (states0-128 are at origin) in x_2 - y_2 plane

3. FINITE STATE PREDICTIVE COMMON MODE VOLTAGE CONTROL

Common mode voltage can be controlled by prior selection of the space vectors of a seven-phase voltage source inverter when implementing the finite set predictive control. In a seven-phase VSI, the possible switching combinations are (top switches):

- 1-ON, 6-OFF,
- 2-ON, 5-OFF,
- 3-ON, 4-OFF,
- 4-ON, 5-OFF,
- 5-ON, 2-OFF, and
- 6-ON, 1-OFF.

Each switching combination produces different space vectors and also different common mode voltages as listed in Table 1.

It is observed from Table 1, that the common mode voltage magnitude varies with the choice of space vectors. The common mode voltage magnitude and different switch combinations are given in Table 2. Using zero switching states (all upper switches ON or all lower switches ON) produced either zero common mode voltage or highest common mode voltage. In all common mode voltage reduction techniques generally, use of zero vector is avoided. In order to maintain the common mode voltage constant so that common mode current remains zero the set of vectors that can be used can be chosen from Table 2. In order to obtain maximum output voltage it is mandatory to use large lengths space vectors. However, if 14 largest vectors are used the common mode voltage will vary between $4/7V_{dc}$ and $3/7V_{dc}$. Hence any one set of seven largest length vectors can be used to implement finite set predictive control.

Table 1. Switching combinations and common mode voltages in a seven-phase VSI

Vector Number	Switching combination	Common mode voltage
1st Large Vectors $(7\cos(3\pi/7))^{-1}V_{DC} \cong 0.6420V_{DC}$		
97, 112, 56, 28, 14, 7, 67,	{1100001}, {1110000}, {0111000}, {0011100}, {0001110}, {0000111},	$(3/7)V_{dc}$
	{1000011}	
113, 120, 60, 30, 15, 71,	{1110001}, {1111000}, {0111100}, {0011110}, {0001111}, {1000111},	$(4/7)V_{dc}$
99	{1100011}	
2nd Large Vectors $(4/7)\cos(\pi/7)V_{DC} \cong 0.5148V_{DC}$		
115, 121, 124, 62, 31, 79,	{1110011}, {1111001}, {1111100}, {0111110}, {0011111}, {1001111},	$(5/7)V_{dc}$
103	{1100111}	
96, 48, 24, 12, 6, 3, 65	{1100000}, {0110000}, {0011000}, {0001100}, {0000110}, {0000011},	$(2/7)V_{dc}$
	{1000001}	
3rd Large Vectors $(4/7)V_{DC} \cong 0.4041V_{DC}$		
81, 104, 52, 26, 13, 70, 35,	{1010001}, {1101000}, {0110100}, {0011010}, {0001101}, {1000110},	$(3/7)V_{dc}$
49, 88, 44, 22, 11, 69, 98	{0100011}, {0110001}, {1011000}, {0101100}, {0010110}, {0001011},	
	{1000101}, {1100010}	
114, 57, 92, 46, 23, 75,	{1110010}, {0111001}, {1011100}, {0101110}, {0010111}, {1001011},	$(4/7)V_{dc}$
101, 105, 116, 58, 29, 78,	{1100101}, {1101001}, {1110100}, {0111010}, {0011101}, {1001110},	
39, 83	{0100111}, {1010011}	
4th Large Vectors $(4/7)\cos(2\pi/7)V_{DC} \cong 0.3563V_{DC}$		
33, 80, 40, 20, 10, 5, 66	{0100001}, {1010000}, {0101000}, {0010100}, {0001010}, {0000101},	$(2/7)V_{dc}$
	{1000010}	
117, 122, 61, 94, 47, 87,	{1110101}, {1111010}, {0111101}, {1011110}, {0101111}, {1010111},	$(5/7)V_{dc}$
107	{1101011}	
5th Large Vectors $(2/7)V_{DC} \cong 0.2857V_{DC}$		
64, 32, 16, 8, 4, 2, 1	{1000000}, {0100000}, {0010000}, {0001000}, {0000100}, {0000010},	$(1/7)V_{dc}$
	{0000001}	
123, 125, 126, 63, 95, 111,	{1111011}, {1111101}, {1111110}, {0111111}, {1011111}, {1101111},	$(6/7)V_{dc}$
119	{1110111}	
6th Large Vectors $(7\cos(2\pi/7))^{-1}V_{DC} \cong 0.2291V_{DC}$		
51, 89, 108, 54, 27, 77,	{0110011}, {1011001}, {1101100}, {0110110}, {0011011}, {1001101},	$(4/7)V_{dc}$
102	{1100110}	
100, 50, 25, 76, 38, 19, 73	{1100100}, {0110010}, {0011001}, {1001100}, {0100110}, {0010011},	$(3/7)V_{dc}$
	{1001001}	
7th Large Vectors $(7\cos(\pi/7))^{-1}V_{DC} \cong 0.1586V_{DC}$		
82, 41, 84, 42, 21, 74, 37	{1010010}, {0101001}, {1010100}, {0101010}, {0010101}, {1001010},	$(3/7)V_{dc}$
	{0100101}	
106, 53, 90, 45, 86, 43, 85	{1101010}, {0110101}, {1011010}, {0101101}, {1010110}, {0101011},	$(4/7)V_{dc}$
	{1010101}	
Smallest Vectors $(4/7)\cos(3\pi/7)V_{DC} \cong 0.1272V_{DC}$		
109, 118, 59, 93, 110, 55,	{1101101}, {1110110}, {0111011}, {1011101}, {1101110}, {0110111},	$(5/7)V_{dc}$
91	{1011011}	
17, 72, 36, 18, 9, 68, 34	{0010001}, {1001000}, {0100100}, {0010010}, {0001001}, {1000100},	$(2/7)V_{dc}$
	{0100010}	
Zero Vectors		
0	{0000000}	$(0)V_{dc}$
127	{1111111}	$(1)V_{dc}$

Table 2. Common mode voltages for different switching states

Common mode voltage magnitude	Switch combination (Upper switch position)	Number of space vectors
$1/7V_{dc}$	1 (ON)-6 (OFF)	7
$2/7V_{dc}$	2 (ON)-5 (OFF)	21
$3/7V_{dc}$	3 (ON)-4 (OFF)	35
$4/7V_{dc}$	4 (ON)-3 (OFF)	35
$5/7V_{dc}$	5 (ON)-2 (OFF)	21
$6/7V_{dc}$	6 (ON)-1 (OFF)	7

When 7 largest vectors will be used to implement FSPC, the dc link voltage will not be utilized fully. There will be a reduction in the output voltage magnitude and hence the resulting current through the load. The drop in the output voltage magnitude can be found using Figure 6.

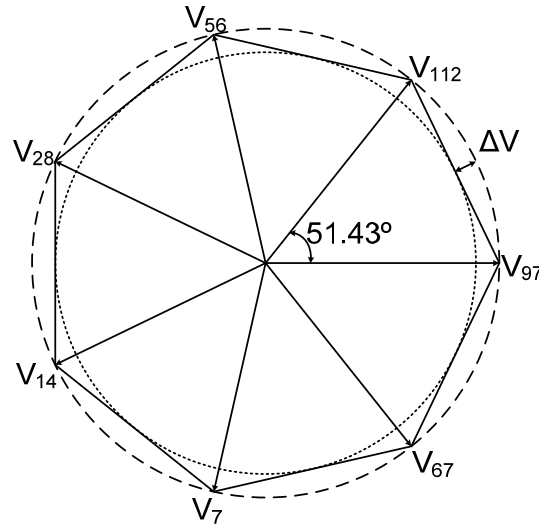


Figure 6. Locus of the output voltage in a seven-phase VSI

The maximum output voltage when 14 largest length vectors are used is same as the radius of the inscribed circle. The reduction in the output voltage magnitude can thus be calculated as:

$$\begin{aligned}
 V_{out} &= |V| \cos\left(\frac{25.7}{2}\right) - |V| \cos\left(\frac{51.4}{2}\right) \\
 &= 0.626V_{dc} - 0.5785V_{dc} = 0.0475V_{dc}
 \end{aligned} \tag{6}$$

In this section, it is explained the results of research and at the same time is given the comprehensive discussion. Results can be presented in figures, graphs, tables and others that make the reader understand easily [2], [5]. The discussion can be made in several sub-chapters.

4. SIMULATION RESULTS

Simulation is carried out for two possible solutions in Matlab/Simulink environment, nevertheless, many more can be evaluated. Following cases are considered:

- 14 large space vectors and one zero space vector (0000000)
- 14 large space vectors only
- 7 large space vectors and one zero space vector (0000000)
- 7 large space vectors only

Investigation is done at first using outer large vectors set (14 active vectors and one zero vector) from Table 2. The tuning parameters are set such that x_1 - y_1 and x_2 - y_2 plane vectors are eliminated and sinusoidal current is produced. Common mode voltage varies between zero, $3/7V_{dc}$ and $4/7V_{dc}$. Further to obtain common mode voltage between two levels i.e. $3/7V_{dc}$ and $4/7V_{dc}$, zero vector is not employed and only 14 large space vectors are chosen. The third case is considered when only 8 space vectors (7 large active space vector and one zero vector) are used such that common mode voltage varies between 0 is $3/7V_{dc}$. Further to obtain constant common mode voltage only 7 large active space vectors are chosen. The fundamental frequency of the sinusoidal reference current is chosen as 30 Hz. The load parameters are $R = 75 \Omega$, $L = 33 \text{ mH}$ and $E = 0$, and the dc link voltage is kept at $V_{dc} = 600 \text{ V}$. The seven-phase reference current amplitude is at first kept at 3.0 A and then is stepped up to 4.0 A and further reduced to 2.0 A. The sampling time of algorithm is kept at 20 μ Sec. The optimization algorithm is implemented using 's' function of the Matlab/Simulink.

Case 1: Using 14 Largest space vectors and one zero vector with $\mu=1$, $\gamma=1$, $\delta=1$

The simulation is carried out with fourteen active and one zero vector while the cost function minimizes current tracking error in all the three orthogonal planes. This is achieved by keeping the tuning parameters

$\mu = 1, \gamma = 1, \delta = 1$. This results in a control action in all planes. The sampling time of the algorithm is kept at 20 μsec , which is reasonable for processor handling. The resulting waveforms are shown in Figure 8 for phase 'a' actual and reference current, the transformed currents ($d-q$, x_1-y_1 and x_2-y_2), the spectrum of phase 'a' current and common mode voltage. The vectors that are used for implementing the model predictive control is elaborated in Figure 7, where the vectors in all three planes are depicted.

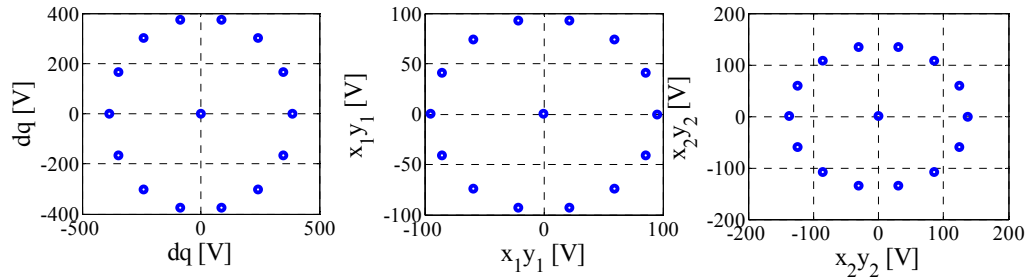


Figure 7. Fourteen large vectors and one zero and their mapping

The actual current follows well the reference current with fast dynamics. The Total harmonic distortion is 6.52% considering the computation upto 50th harmonics. The voltage vectors of $d-q$ plane is dominant and the other two planes are killed in order to obtain sinusoidal output currents. Common mode voltage varies between zero, $3/7V_{dc}$, $4/7V_{dc}$. The dv/dt is large either $3/7V_{dc}$ or $4/7V_{dc}$.

Case 2: Using 14 Largest space vectors with $\mu=1, \gamma=1, \delta=1$

The simulation is carried out with fourteen largest lengths active space vectors while the cost function minimizes current tracking error in all the three orthogonal planes. This is achieved by keeping the tuning parameters $\mu = 1, \gamma = 1, \delta = 1$. This results in a control action in all planes. The sampling time of the algorithm is kept same at 20 μsec as in the previous case. The resulting waveforms are shown in Figure 9 for phase 'a' actual and reference current, the transformed currents ($d-q$, x_1-y_1 and x_2-y_2), the spectrum of phase 'a' current and common mode voltage.

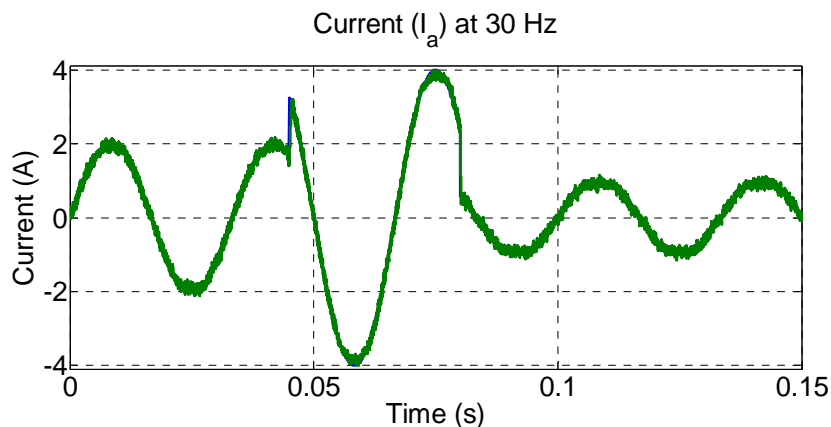


Figure 8a. Actual and reference phase 'a' current

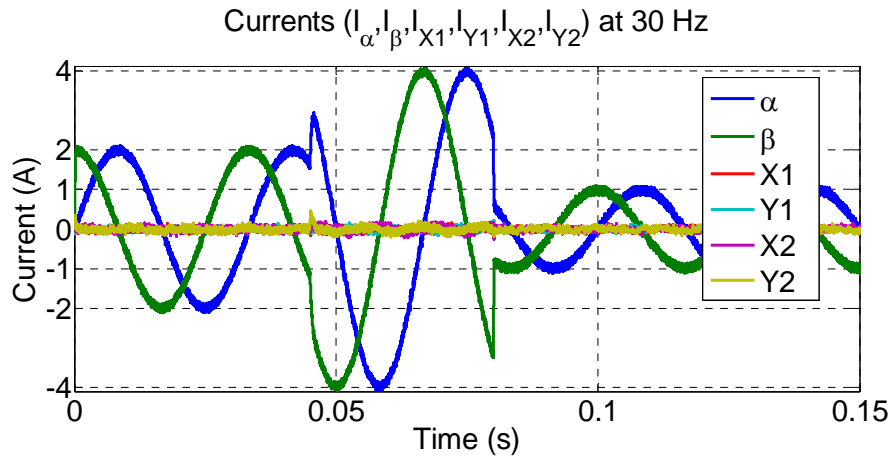


Figure 8b. Transformed currents in $d-q$, x_1-y_1 and x_2-y_2 planes.

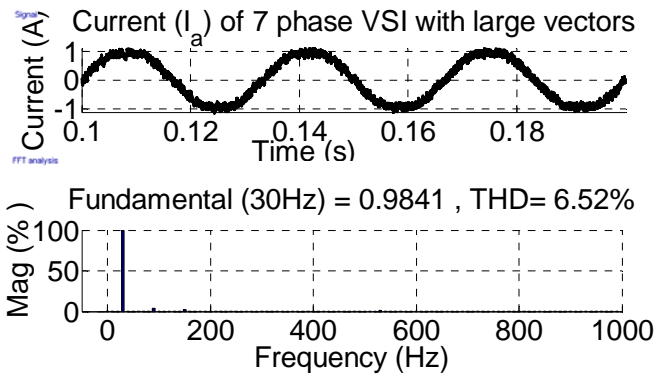


Figure 8c. Phase 'a' current time domain and frequency domain plots

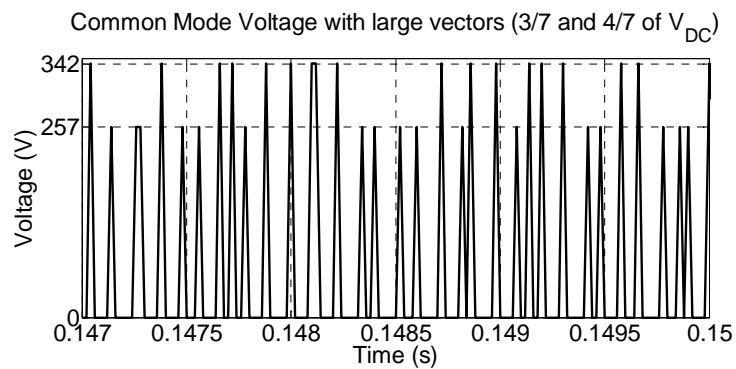


Figure 8d. Common mode voltage

The common mode voltage is seen to vary between two levels which $3/7V_{dc}$ and $4/7V_{dc}$. The dv/dt is much reduced is now $1/7V_{dc}$.

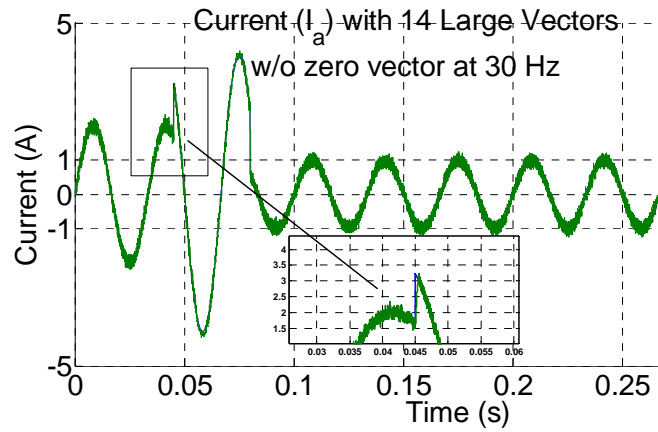


Figure 9a. Actual and reference phase 'a' current

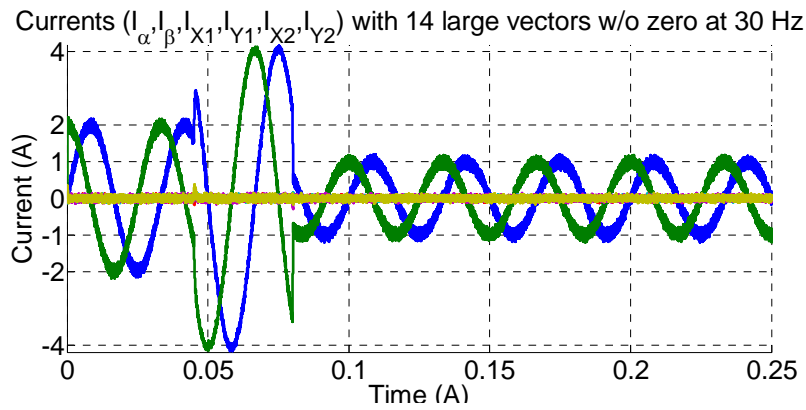


Figure 9b. Transformed currents in d - q , x_1 - y_1 and x_2 - y_2 planes

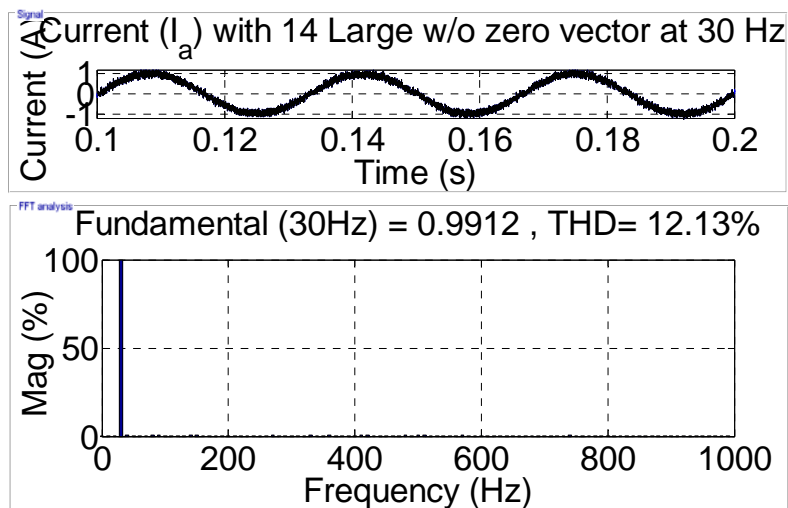


Figure 9c. Phase 'a' current time domain and frequency domain plots

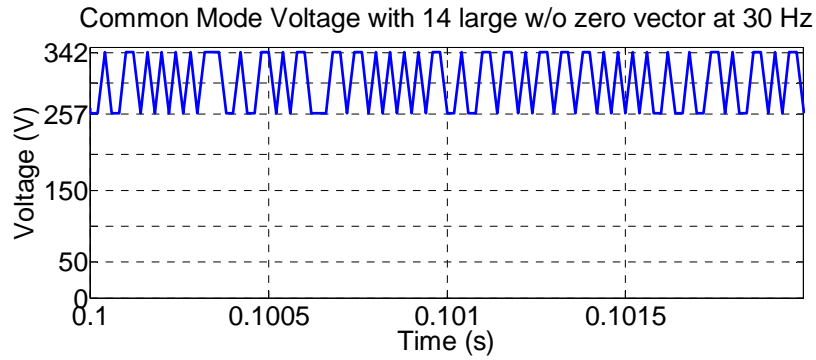


Figure 9d. Common mode voltage

Case 3: Using 7 Largest space vectors and one zero space vector with $\mu=1, \gamma=1, \delta=1$

The simulation is carried out with 7 largest lengths active space vectors and one zero vectors (0000000), while the cost function minimizes current tracking error in all the three orthogonal planes. This is achieved by keeping the tuning parameters $\mu=1, \gamma=1, \delta=1$. This results in a control actions in all planes. The sampling time of the algorithm is kept same at 20 μsec as in the previous case. The resulting waveforms are shown in Figure 10 for phase 'a' actual and reference current, the transformed currents ($d-q, x_1-y_1$ and x_2-y_2), the spectrum of phase 'a' current and common mode voltage. The THD is observed to increase to almost 15%. The common mode voltage is seen to vary between two zero and $3/7V_{dc}$ and hence the dv/dt is also $3/7V_{dc}$.

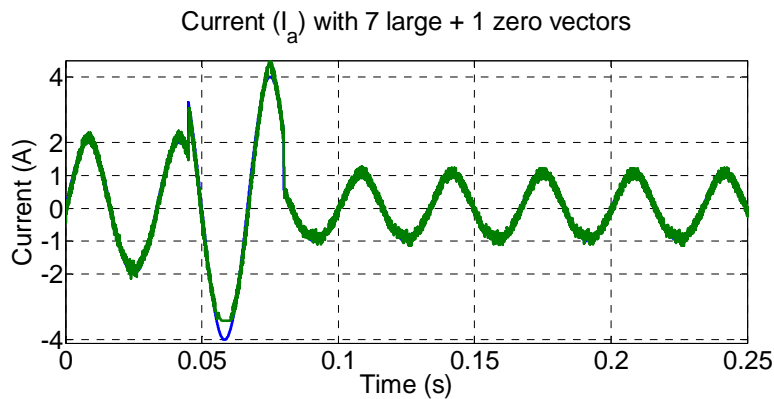


Figure 10a. Actual and reference phase 'a' current

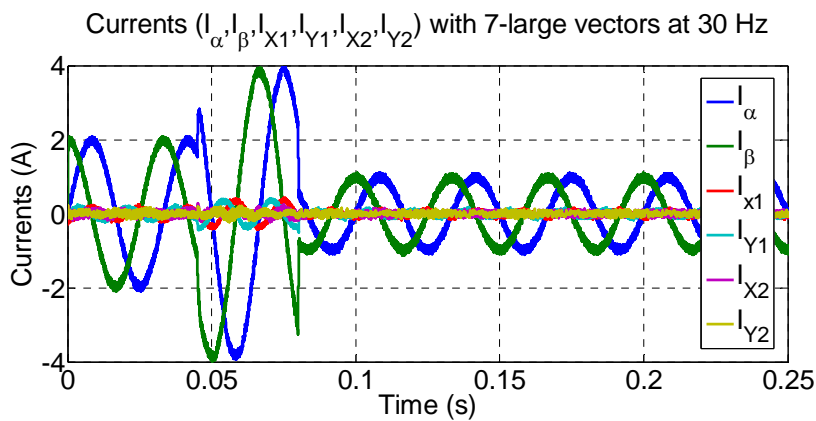


Figure 10b. Transformed currents in $d-q, x_1-y_1$ and x_2-y_2 planes

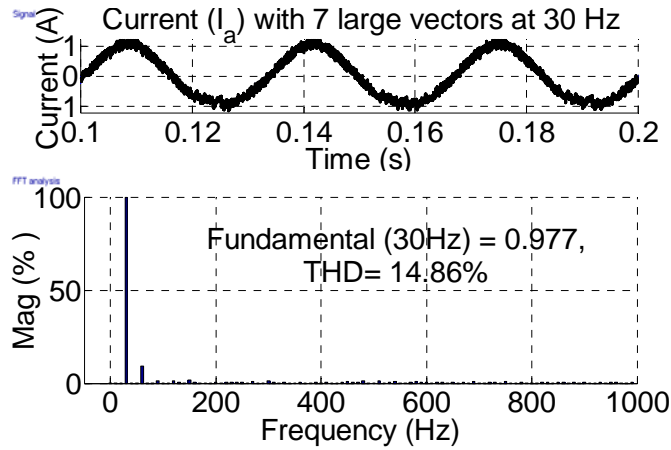


Figure 10c. Phase ‘a’ current time domain and frequency domain plots.

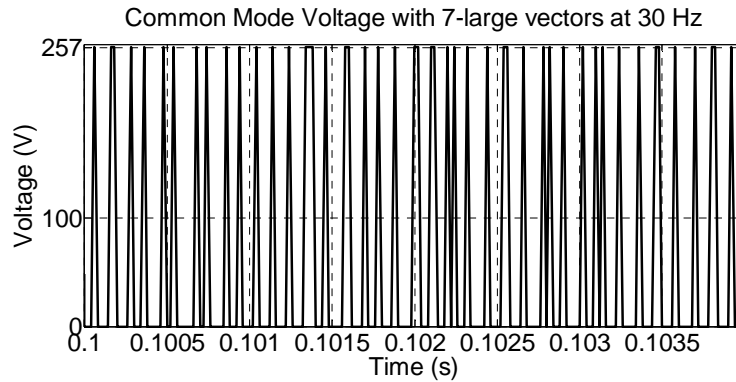


Figure 10d. Common mode voltage

Case 4: Using 7 Largest space vectors with $\mu = 1, \gamma = 1, \delta = 1$

The simulation is carried out with 7 largest lengths active space vectors, while the cost function minimizes current tracking error in all the three orthogonal planes. This is achieved by keeping the tuning parameters $\mu = 1, \gamma = 1, \delta = 1$. This results in control actions in all the planes. The sampling time of the algorithm is kept same at 20 μ sec as in the previous case. The resulting waveforms are shown in Figure 11 for phase ‘a’ actual and reference current, the transformed currents ($d-q, x_1-y_1$ and x_2-y_2), the spectrum of phase ‘a’ current and common mode voltage. The actual current tracks the reference very well. The unwanted x_1-y_1 and x_2-y_2 components remains zero. The common mode voltage is seen to remain constant.

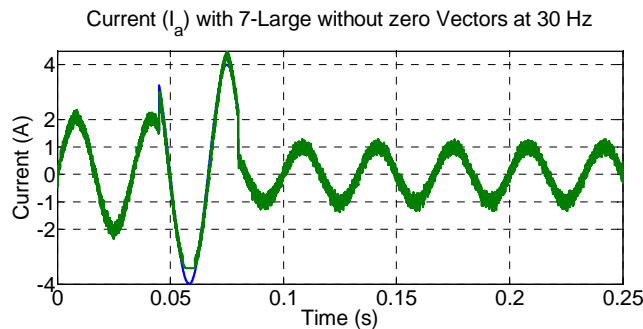


Figure 11a. Actual and reference phase ‘a’ current

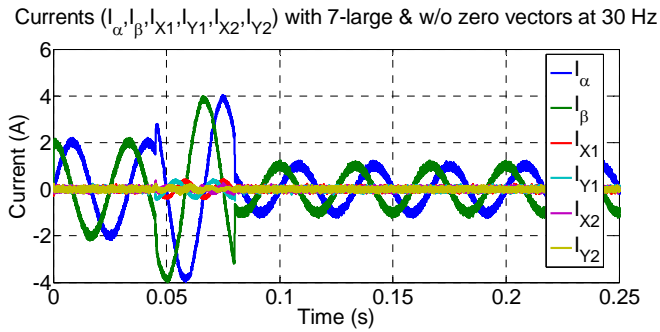
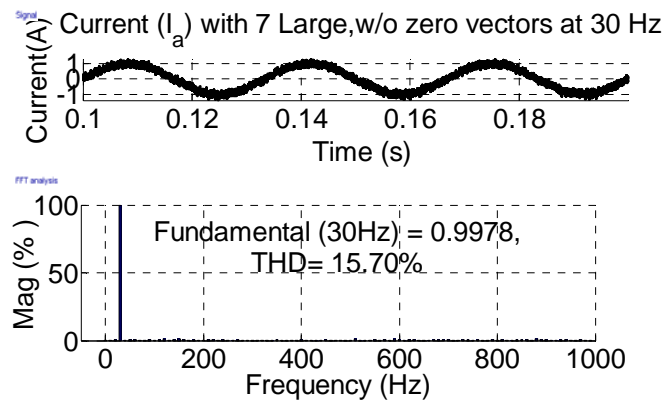
Figure 11b. Transformed currents in d - q , x_1 - y_1 and x_2 - y_2 planes

Figure 11c. Phase 'a' current time domain and frequency domain plots

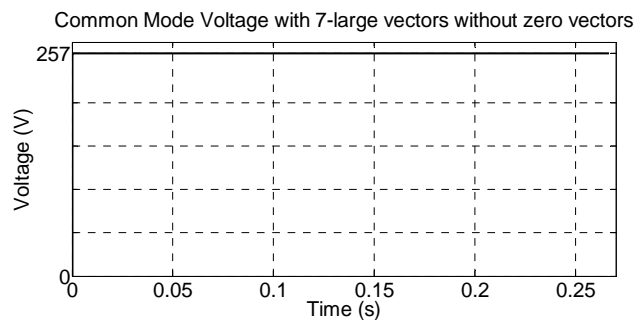


Figure 11d. Common mode voltage

5. EXPERIMENTAL RESULTS

An experimental prototype seven-phase voltage source inverter is developed in the laboratory. The seven-phase inverter is controlled from dSpace 1006 in conjunction with FPGA card DS 5203. The dSpace processor is connected with the FPGA card using PHS bus system. The control algorithm is written in the processor and the PWM signals are generated in the FPGA card using System Generator. A dead band circuit is formulated outside the dSpace board based on FPGA and a dead band of $2 \mu\text{s}$ is created using VHDL. Sample time of $20 \mu\text{s}$ is used and a reference current of 2 A is chosen which is then stepped down to 1 A with load impedance $R = 75 \Omega$ and $L = 33 \text{ mH}$ and in one case the current is increased from 1 A to 2 A. For experimental purpose, 7 space vectors are employed with control action on all three planes. The resulting waveform is shown in Figure 12. The reference and actual currents are plotted in one waveform. A high dynamics of the control is evident and also a good tracking is obtained. The common mode voltage is maintained at constant value. This proves the viability of the proposed control.

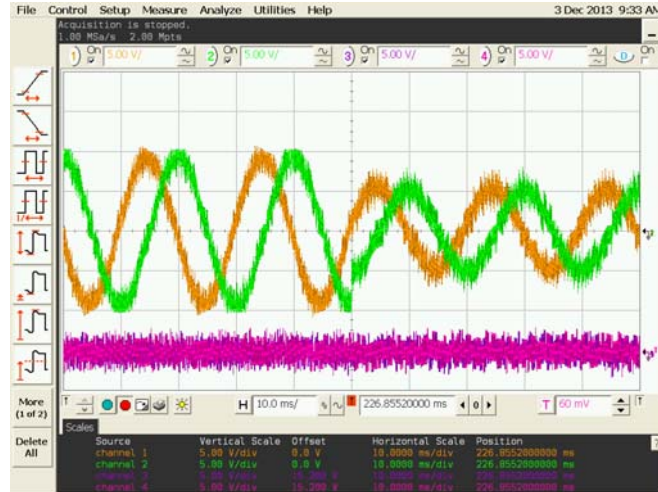


Figure 12a. Transformed currents

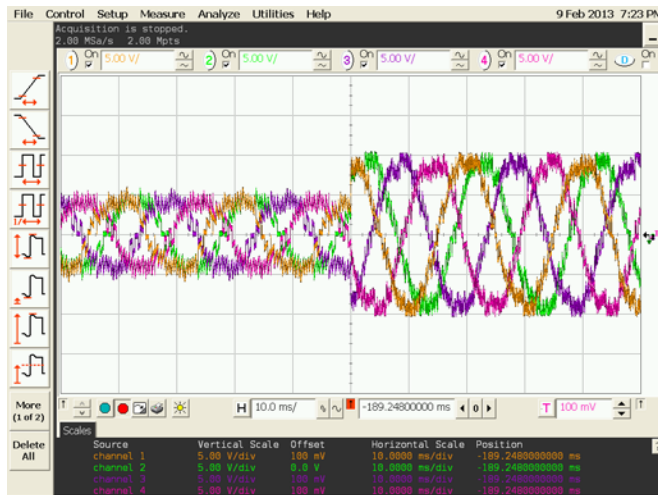


Figure 12b. Step change for phases A-C-E-G

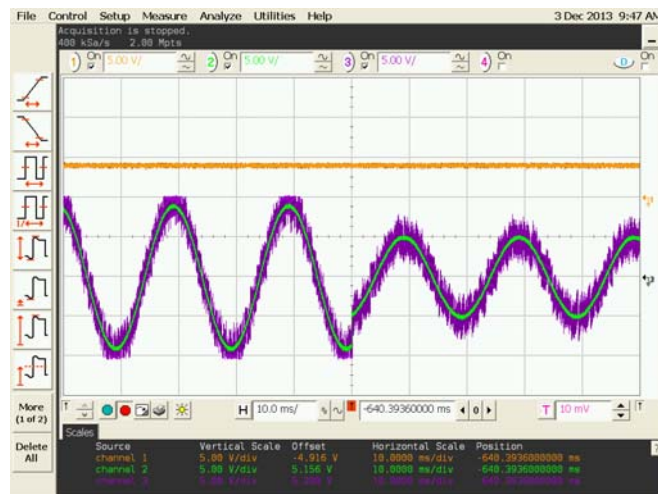


Figure 12c. Common mode voltage and phase 'a' current

6. CONCLUSION

The paper proposes current control technique based on finite set model predictive current and common mode voltage control of a seven-phase voltage source inverter. The discrete time model of the load is used to predict the future behavior of the load current required in the next sampling interval. Space vector model of a seven-phase VSI is elaborated and out of 128 space vectors, four different scenario are investigated; a) 15 space vectors with control actions in all three planes. This shows three levels of common mode voltage. The current THD is reasonably small. b) 14 space vectors with control in three planes. The common mode voltage now has only two levels and hence the dv/dt is significantly reduced. c) 8 space vector are employed which yield again two level common mode voltage with good tracking of actual phase currents. The rate of change of voltage is considerably high and so the THD. d) 7 space vectors are used without zero vector and hence constant common mode voltage is obtained with good tracking ability. The simulation and experimental results matches very well. The effect of dead time will be further investigated.

Acknowledgement

This publication was made possible by NPRP grant [4 - 077 - 2 – 028] from the Qatar National Research Fund (a member of Qatar Foundation). The statements made herein are solely the responsibility of the authors.”

REFERENCES

- [1] G.D. Holmes and T.A. Lipo, “*Pulse Width Modulation for Power Converters - Principles and Practice*”, IEEE Press Series on Power Engineering, John Wiley and Sons, Piscataway, NJ, USA, 2003.
- [2] M.P Kazmierkowski, R. Krishnan and F. Blaabjerg, “*Control in Power Electronics Selected Problems*”, Academic Press, 2002.
- [3] R. Ramchand, K. Gopakumar, C. Patel, K. Sivakumar, A. Das, and H. Abu-Rub “Online Computation of Hysteresis Boundary for Constant Switching Frequency Current-Error Space-Vector-Based Hysteresis Controller for VSI-Fed IM Drives”, *IEEE Trans. On Power Electronics* vol. 27, no. 3, pp. 1521-1529, March 2012.
- [4] A. Linder and R. Kennel, “Model Predictive control for electric Drives”, *Proc. 36th Annual IEEE PESC*, Recife, Brazil, pp. 1793-1799, 2005.
- [5] H. Abu-Rub, J. Guzinski, Z. Krzeminski and H. A. Toliyat, “Predictive current control of a voltage source inverters”, *IEEE Trans. On Ind. Elect.*, vol. 51, no. 3, pp. 585-593, June 2004
- [6] P. Cortes, P. Kazmierkowski, R.M. Kennel, D. E. Quevedo and J. Rodriguez, “Predictive control in Power Electronics and Drives”, *IEEE Trans. On Ind. Elect.*, vol. 55, no. 12, pp. 4312-4321, Dec. 2008.
- [7] J. Rodriguez and P. Cortes, “*Predictive control of Power converters and electric drives*”, Wiley, UK., 2012.
- [8] J.H. Lee, “Model predictive control: Review of three decades of development”, *Int. journal of Control Automation and System*, vol. 9, no. 3, pp. 415-424, 2011.
- [9] M. Jones and E. Levi, “A literature survey of state-of-the-art in multiphase ac drives”, *Proc. 37th Int. Universities Power Eng. Conf. UPEC*, Stafford, UK, 2002, pp. 505-510.
- [10] A. Iqbal, H. Abu-Rub, SK. M. Ahmed, P. Cortes, and J. Rodriguez, “Finite state model predictive control of a five-phase VSI”, *Proc. IEEE ICIT*, 2010.
- [11] A. Iqbal, H. Abu-Rub, SK. M. Ahmed, P. Cortes, and J. Rodriguiz, “Model Predictive current control of a two-level five-phase voltage source inverter”, *Int. Journal of Applied Engineering Research*, vol. 5, no. 21, pp. 3503-3514, 2010.
- [12] F. Barrero, M.R. Arahal, R. Gregor, S. Toral and M.J. Duran, “A Proof of concept study of Predictive current control for VSI Driven Asymmetrical Dual three-phase AC machines”, *IEEE Tran. On Ind. Elect.* Vol. 56, no. 6, pp. 1937-1954, June 2009.
- [13] M.R. Arahal, F. Barrero, S. Toral, M. Duran and R. Gregor, “Multi-phase current control using finite state model predictive control”, *Control Engg. Practice*, vol. 17, pp. 579-587, 2009.
- [14] F. Barrero, M.R. Arahal, R. Gregor, S. Toral and M. Duran, “One Step Modulation Predictive current control method for asymmetrical dual three-phase induction machine”, *IEEE Trans. On Ind. Elect.* Vol. 56, no.
- [15] J. Prieto, F. Barrero, M. Jones, and E. Levi, “A modified continuous PWM technique for asymmetrical six-phase induction machines”, *Proc. IEEE Int. Conf. on Ind. Tech. ICIT*, pp. 1489-1494, 2010.
- [16] A. Iqbal, H. Abu-Rub, SK. M. Ahmed, P. Cortes, and J. Rodriguez, “Finite state model predictive control of a three-level five-phase NPC inverter”, *Proc. IEEE 36th IECON*, pp. 2953-2958, 2010.
- [17] A. Iqbal, K. Rahman, M. Mostafa, A.A. Abdullah, H. Abu-Rub. “Model predictive control of a seven-phase voltage source inverter”, *Int. Conf., on Advances in Power Electronics and Instrumentation Engineering*, 01-02 Aug. 2013 Chandigarh, India, pp. 6-12, DOI: 03.LSCS.2013.4.
- [18] E. Levi, “Multi-phase Machines for variable speed applications”, *IEEE Trans. On Ind. Elect.* vol. 55, no. 5, May 2008, pp. 1893-1909.
- [19] A. Iqbal and E. Levi, “Space vector PWM techniques for sinusoidal output voltage generation with a five-phase voltage source inverter”, *Electric Power components and system*, vol. 34, no. 2, 2006, pp. 119-140.
- [20] A. Iqbal, SK. M. Ahmed, H. Abu-Rub, A. Jidin, “Current control of a five-phase VSI”, *Int. Conf. ICPEA*, Djelfa, Algeria, Nov., 2013, Paper ID 182.

- [21] A. Iqbal, R. Al-ammari, M. Mostafa, H. Abu-Rub, "Finite Set Model Predictive Current Control with Reduced and Constant Common Mode Voltage for a Five-phase Voltage Source Inverter", *IEEE Int. Symposium on Ind. Elect. ISIE, 1-4 June, 2014, Istanbul, Turkey*, pp. 479-485.
- [22] S. Moinuddin and A. Iqbal, "Analysis of Space vector PWM techniques for a seven-phase VSI", *I-Manger Journal of Engineering and Technology*, vol. 1. No. 2., pp. 53-63, Oct-Dec. 2007
- [23] S. Moinuddin, and A. Iqbal, "Modelling and Simulation of a seven-phase voltage source inverter", *I-Manger Journal of Engineering and Technology*, vol. 1, no. 1, July-Sept 2007, pp. 30-41.

BIOGRAPHIES OF AUTHORS



Atif Iqbal, Senior Member IEEE, PhD (UK)- Associate Professor at the Dept. of Electrical Engineering, Qatar University, Doha, Qatar and Full Professor at the Dept. of Electrical Engineering, Aligarh Muslim University, Aligarh, India. Recipient of Outstanding Faculty Merit Award AY 2014-2015 and Research excellence award at Qatar University, Doha, Qatar. He received his B.Sc. (Gold Medal) and M.Sc. Engineering (Electrical) degrees in 1991 and 1996, respectively, from the Aligarh Muslim University (AMU), Aligarh, India and PhD in 2006 from Liverpool John Moores University, Liverpool, UK. He has been employed as a Lecturer in the Department of Electrical Engineering, AMU, Aligarh since 1991 where he is currently working as Professor. He is on academic assignment and working as an Associate Professor at the Dept. of Electrical Engineering, Qatar University, Doha, Qatar. Dr. Iqbal has received "Research excellence award" for 2015 in Science & Engineering category at Qatar University, Doha, Qatar. He is recipient of Maulana Tufail Ahmad Gold Medal for standing first at B.Sc. Engg. Exams in 1991 from AMU. He has been given best research papers awards at IEEE ICIT-2013 and IET-SESICON-2013. He has published widely in International Journals and Conferences his research findings related to Power Electronics and Renewable Energy Sources. Dr. Iqbal has authored/co-authored more than 240 research papers and one book and two chapters in two other books. He has supervised several large R&D projects. He is also a Principle Investigator in one of the largest projects funded by Qatar Foundation on grid integration of Solar Photovoltaic System to the utility grid without a transformer. His principal area of research interest is Modeling and Simulation of Power Electronic Converters, Control of multi-phase motor drives and Renewable Energy sources.



Shaikh Moinoddin (M'10) received the B.E. and M.Tech. (electrical) degrees and the Ph.D. degree in multiphase inverter modeling and control, all from the Aligarh Muslim University (AMU), Aligarh, India, in 1996, 1999, and 2009, respectively. He served in the Indian Air Force from 1971 to 1987. He has been with the University Polytechnic, AMU, since 1987, where he is currently an Assistant Professor. He was a Postdoctoral Research Associate and Assistant Research Scientist at Texas A&M University at Qatar, Doha, Qatar. His principal research interests include power electronics and electric drives. Dr. Moinoddin received the University Gold Medals for standing first in the electrical branch and in all branches of engineering during the B.E. 1996 exams.



Khaliqur Rahman received the B.Tech and M.Tech. degrees from Aligarh Muslim University (AMU), Aligarh, India, in 2008 and 2010, respectively. He is a PhD student in Qatar University, Doha, Qatar. From 2010 to 2012, he worked as a Lecturer (Guest Faculty) in Aligarh Muslim University, Aligarh, India. From Sep-2012 to March-2015 he was engaged in a research assignment at Qatar University, Qatar. His principal areas of research are modeling, simulation, and control of multi-phase power electronic converters, particularly matrix converters and multiphase drives.